The Angles between the C_1−, C_5−, and C_9−Methyl Bonds of the Retinylidene Chromophore and the Membrane Normal Increase in the M Intermediate of Bacteriorhodopsin: Direct Determination with Solid-State ^{2}H NMR†

Stephan Moltke,‡,§ Ingrid Wallat,|| Naomi Sakai,⊥ Koji Nakanishi,⊥ Michael F. Brown,‡ and Maarten P. Heyn*,||,#

Departments of Chemistry and Biochemistry, University of Arizona, Tucson, Arizona 85721, Department of Physics, Freie Universität Berlin, Arnimallee 14, D-14195 Berlin, Germany, and Department of Chemistry, Columbia University, New York, New York 10027

Received March 16, 1999; Revised Manuscript Received June 15, 1999

ABSTRACT: The orientations of three methyl bonds of the retinylidene chromophore of bacteriorhodopsin were investigated in the M photointermediate using deuterium solid-state NMR (^{2}H NMR). In this key intermediate, the chromophore has a 13-*cis*, 15-*anti* conformation and a deprotonated Schiff base. Purple membranes containing wild-type or mutant D96A bacteriorhodopsin were regenerated with retinals specifically deuterated in the methyl groups of either carbon C_1 or C_5 of the β-ionone ring or carbon C_9 of the polyene chain. Oriented hydrated films were formed by drying concentrated suspensions on glass plates at 86% relative humidity. The lifetime of the M state was increased in the wild-type samples by applying a guanidine hydrochloride solution at pH 9.5 and in the D96A sample by raising the pH. ^{2}H NMR experiments were performed on the dark-adapted ground state (a 2:1 mixture of 13-*cis*, 15-*syn* and *all-trans*, 15-*anti* chromophores), the cryotrapped light-adapted state (*all-trans*, 15-*anti*), and the cryotrapped M intermediate (13-*cis*, 15-*anti*) at −50 °C. Bacteriorhodopsin was first completely converted to M under steady illumination of the hydrated films at +5 °C and then rapidly cooled to −50 °C in the dark. From a tilt series of the oriented sample in the magnetic field and an analysis of the ^{2}H NMR line shapes, the angles between the individual $C-CD_3$ bonds and the membrane normal could be determined even in the presence of a substantial degree of orientational disorder. While only minor differences were detected between dark- and light-adapted states, all three angles increase in the M state. This is consistent with an upward movement of the C_5-C_{13} part of the polyene chain toward the cytoplasmic surface or with increased torsional strain. The C_9-CD_3 bond shows the largest orientational change of 7° in M. This reorientation of the chromophore in the binding pocket provides direct structural support for previous suggestions (based on spectroscopic evidence) for a steric interaction in M between the C_9−methyl group and Trp 182 in helix F.

Solving the structure of proteins in functionally important intermediate states of their reaction sequence is a key problem in understanding the mechanism of catalysis. In the case of the light energy converter bacteriorhodopsin (bR),[1] several intermediates are known to occur during the photocycle triggered by the absorption of a photon of visible light (for a review see ref *1*). Its retinylidene chromophore, bound via a protonated Schiff base to lysine 216 of bacterioopsin (cf. Figure 1), isomerizes from *all-trans*, 14-s-*trans*, 15-*anti* in the bR_{all-t} ground state (*2*, *3*) to 13-*cis* in a few picoseconds and is found as a 13-*cis*, 14-s-*trans*, 15-*anti* isomer in the L intermediate (*4*, *5*). In the transition from L to M, the Schiff base deprotonates, but the chromophore configuration remains unchanged (*3*, *6*, *7*). This proton transfer to aspartate 85 constitutes the first major charge translocation during the photocycle. Within the lifetime of M, the so-called "reprotonation switch" is believed to occur: a change in accessibility of the Schiff base from the extracellular to the cytoplasmic side of the membrane. Even after reprotonation of the Schiff base from the internal donor aspartic acid 96, the chromophore configuration is still unchanged in the N state (*8*). The reisomerization to the initial *all-trans*, 14-s-*trans*, 15-*anti* form is observed in the transition from the N to the O intermediate. In the dark, bR_{all-t} exists in a 1:2 equilibrium with another isomeric form,

† Work supported by grants from the National Institutes of Health (GM 53484 to M.P.H., EY 12049 to M.F.B., and GM 36564 to K.N.) and a postdoctoral fellowship from the Deutsche Forschungsgemeinschaft (to S.M.).

* Author to whom correspondence should be addressed: Fachbereich Physik, Freie Universität Berlin, Arnimallee 14, D-14195 Berlin, Germany. Phone: 49-30-838 6141. Fax: 49-30-838 6299. E-mail: heyn@physik.fu-berlin.de.

‡ Department of Chemistry, University of Arizona.

§ Present address: Forschungszentrum Jülich, IBI-2, D-52425 Jülich, Germany.

|| Freie Universität Berlin.

⊥ Columbia University.

Department of Biochemistry, University of Arizona.

[1] Abbreviations: bR, bacteriorhodopsin; bR_{all-t}, light-adapted bR with an *all-trans* chromophore; bR_{13-c}, bR with a 13-*cis* chromophore which coexists in a 2:1 ratio with bR_{all-t} in the dark; D, deuterium; D96A, bacteriorhodopsin mutant with aspartate at position 96 replaced by alanine; FWHM, full width at half-maximum; GuaHCl, guanidine hydrochloride; ^{2}H NMR, deuterium nuclear magnetic resonance spectroscopy.

10.1021/bi990593u CCC: $18.00
Published on Web 08/19/1999

bR_{13-c}, which has a 13-*cis*, 14-s-*trans*, 15-*syn* chromophore and does not pump protons.

A fundamental question about the mechanism of photoreceptors in general concerns the transmission of the light-induced structural changes in the chromophore to the protein. How is the energy absorbed in the form of a photon of visible light utilized to accomplish active charge transport, as in bR, or the activation of a receptor such as in rhodopsin or phytochrome? In the retinal proteins bacteriorhodopsin and rhodopsin, isomerization of the chromophore triggers structural changes that are mediated through altered interactions between the chromophore and its protein binding pocket. The molecular details of these events remain unclear. The protruding methyl groups of the chromophore may provide the interaction sites between the chromophore and the side chains of the amino acids lining the binding pocket. For bacteriorhodopsin, it has been suggested that the C_9-methyl group of retinal interacts transiently with tryptophan 182 of helix F (*9*−*11*). The indole ring of W182 is located between the chromophore and the cytoplasmic side of the membrane and, in the dark, is in van der Waals contact with the C_9-methyl group (*12*, *13*). Thus, a reorientation of the polyene chain in that direction would change the van der Waals interactions between these groups and could serve as the steric trigger leading to the tilt of helix F observed in the M state (*14*−*16*). Alternatively, the torsional strain in the polyene chain after isomerization could drive conformational changes in the protein moiety, with the methyl groups providing the van der Waals contacts. In either case, changes in orientation of the individual $C-CD_3$ bonds are expected to be involved. Here, we report on a substantial increase in the angle between the C_9-CH_3 bond of the chromophore and the membrane normal in M using ^{2}H solid-state NMR.

Although the isomeric configuration of the retinal chromophore in each of the photocycle intermediates is well-known (*1*), structural information on its orientation with respect to the protein or the membrane during the dark reactions is almost completely lacking. Using deuterium NMR (^{2}H NMR) spectroscopy with oriented purple membrane films, the ground state orientations of all three methyl bonds on the polyene chain of the retinal have been measured with high precision (*17*). The same method has also been applied to bacteriorhodopsin containing a retinal stereospecifically labeled in one of the two geminal methyl groups (1*R*-[1-CD_3]) of the cyclohexene ring (*18*). From the orientational constraints provided by these ^{2}H NMR results and in conjunction with structural information from other methods, it was concluded that the polyene methyls point toward the cytoplasmic side and the Schiff base N−H bond points to the extracellular side (*18*). It was also found that the plane of the conjugated system is nearly perpendicular to the membrane surface within 30° (*18*), in good agreement with FTIR results on the hydrogen out-of-plane vibrational modes (*19*−*21*).

In the M state, it was shown with two-dimensional neutron diffraction that the cyclohexene ring does not change its in-plane position, but the Schiff base end moves approximately 1.4 Å toward the ring in the projected density (*22*). This was interpreted as a tilt of the C_5-C_{13} vector out of the membrane plane. The angle between the transition dipole moment and the membrane normal also decreases by 3° in the M state (*23*, *24*). In order to gain deeper insight into the vectoriality of proton transport and the interaction of the isomerized retinal with the binding pocket, more specific information about the chromophore reorientation is needed.

In the present work, we have further developed an approach that uses the angular dependence of the quadrupolar splittings in solid-state deuterium NMR of oriented samples to measure the angles between specifically deuterated bonds of the retinylidene chromophore and the membrane normal in the M state (*25*). The M intermediate is most interesting, not only because it is produced by the deprotonation of the Schiff base to the internal acceptor aspartate 85 but also since major conformational changes involving helices F and G have been documented (*14*−*16*). Moreover, it is believed that during its lifetime the accessibility of the Schiff base for protons changes from the extracellular to the cytoplasmic side of the membrane (the so-called reprotonation switch).

NMR investigations on M require that the uniaxially oriented purple membrane samples stay in this bleached state for the duration of the experiment. The lifetime of the M intermediate can be substantially increased at room temperature by addition of a guanidine hydrochloride solution at pH 9.5 to films with wild-type bR (*26*) or by using the mutant protein D96A, in which the proton donor aspartic acid 96 is replaced by alanine (*27*), at high pH. In both preparations, bR is fully functional and only the turnover of the proton pump is slowed down. Thus, at 86% relative humidity an oriented film of membranes could be converted from the purple ground state to the brightly yellow M state (λ_{max} = 410 nm) at temperatures above freezing, ensuring that bR was fully functional. Thereafter, the sample was rapidly frozen at −50 °C to maintain it in the M state for the duration of the experiment, which in the present case could last up to several days.

Given the increasing evidence for multiple M states, the question arises as to which M state was observed under our experimental conditions. A recent study (*28*) has presented evidence for two structurally different M species at low and at high relative humidity, respectively, which were generated under steady-state illumination of films similar to those employed here. Whereas the low-humidity films showed the characteristics of M, e.g., a deprotonated Schiff base, the tertiary structure differences known to occur in GuaHCl trapped samples (*14*, *15*) were not observable. Only at higher humidities did they appear. The authors reported that the M states trapped in D96N or in GuaHCl-treated wild-type samples at high humidities were identical (*28*). Consequently, the methods of preparing the M state used in the present work (high humidity, +5 °C) most likely trapped the M substate, in which the functionally important protein conformational changes have occurred. Further evidence for this point comes from a recent solid-state NMR study, in which two sequential M intermediates were observed in 0.3 M GuaHCl at pH 10.0 (*29*). Illumination at −10 or −60 °C led to M states with Schiff base ^{15}N chemical shifts which differed by 7 ppm. The M state produced by illumination at the lower temperature decayed upon warming to the second M substate, and this transition was accompanied by a substantial protein conformational change and an increase in the pK_a of the Schiff base (*29*). Since we illuminated our GuaHCl-treated samples at +5 °C, we have presumably also prepared this "post switch" state, in which helix F is tilted (*14*−*16*).

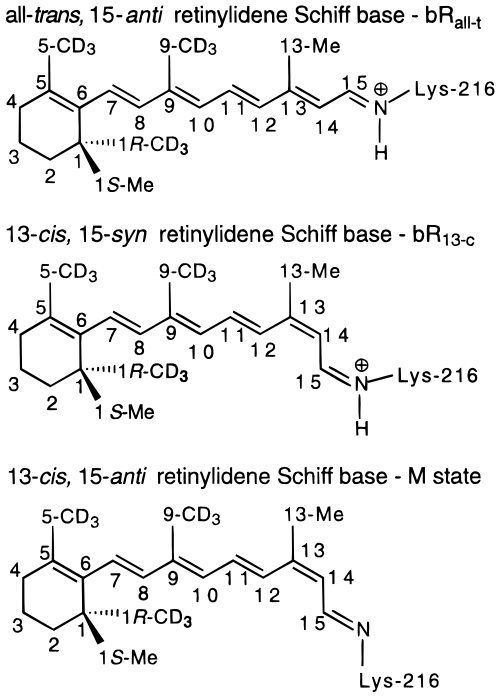

FIGURE 1: Carbon atom numbering for the retinylidene chromophore of bacteriorhodopsin. The three conformations represent the three most important structures as found in purple membranes. The bR_{all-t} ground state (top) is the active form of bacteriorhodopsin. The 13-*cis*, 15-*syn* (middle) conformer occurs in the dark in a 2:1 mixture of bR_{13-c} and bR_{all-t}. In the M state, the chromophore is 13-*cis*, 15-*anti* (bottom), which distinguishes it from the bR_{13-c} form, and the Schiff base is deprotonated. For the present study, retinal was specifically deuterated in one of the three methyl groups indicated (CD_3) in order to avoid overlap of ^2H NMR lines.

For the ^2H NMR experiments presented here, three samples were prepared with retinal specifically deuterated in one of the methyl groups attached to carbons C_5, C_9, or C_1 (cf. Figure 1 for the nomenclature). We investigated how the angles between the respective C−C bond and the membrane normal changed in the transition from the ground to the M state. Since the long lifetime of the M intermediate in these samples allowed a well-defined light adaptation of the sample, and since the samples could be kept in the light-adapted state by freezing (*30*), we report here also for the first time on orientational changes associated with light−dark adaptation. All previous ^2H NMR experiments on the ground state used dark-adapted samples. We observed no significant difference between the ^2H NMR line shapes of dark- and light-adapted samples. The angles between the bonds and the membrane normal are greater in M than in the ground state, indicating an out-of-plane tilt of the retinal or a substantial torsional strain. The difference is small for the bonds on the cyclohexene ring but is 7° for the C_9-CD_3 group. Since the alignment of the individual purple membranes on the plates is reduced by the GuaHCl treatment, the mosaic spread is correspondingly large and a precise and flexible method of analysis is required in order to reliably determine the bond angles from the ^2H NMR line shapes.

MATERIALS AND METHODS

Sample Preparation. The procedures for the specific deuteration of retinal have been described previously for the C_5-CD_3 and C_9-CD_3 groups (*31*, *32*), as well as the stereospecifically labeled 1*R*-[1-CD_3] group (*18*). Purple membranes containing wild-type bR were isolated from *Halobacterium salinarium* strain ET1001 according to standard procedures (*18*, *33*). The point-mutated protein D96A, in which aspartate 96 is replaced by alanine, was expressed in a homologous halobacterial system (*34*) and purified in the same way. Although three different bands of purple membranes are observed for D96A on a sucrose gradient, the entire purple membrane fraction was used. Three milliliters of a highly concentrated suspension of membranes was prepared by centrifugation in deuterium-depleted water. In the case of the D96A mutant protein, the pH of this suspension was adjusted to 12 in order to increase the M state lifetime. The UV−visible absorption spectrum yielded no detectable absorption change at 380 nm, thus assuring that the chromophore did not bleach in the dark at this high pH. The pH in the hydrated films of D96A was clearly less than that of the membrane suspension, as evidenced by the accelerated decay of M. Small aliquots of 100 μL were spread evenly on 0.3 mm thin glass plates over an area of 10 mm length and 5−8 mm width. The films were dried slowly at 86% relative humidity, set by a saturated KCl solution in a closed box. In the highly oriented films, the membranes were aligned parallel to the glass surface. Each sample consisted of approximately 80 mg of protein on 26−32 plates.

After 3 days of drying at 86% relative humidity, 100 μL of a 500 mM guanidine hydrochloride solution (50 mM sodium carbonate buffer at pH 9.5) was spread over the films of wild-type bR, which causes them to swell. The drying was subsequently continued for 3 more days. The GuaHCl-treated films proved to be slightly hygroscopic, and it was necessary to dry the plates for about 20 min in room air before they could be used in an experiment.

At one end of the 30 mm long glass plates a small spacer was glued so that two of them could be put together as a sandwich with the purple membrane films facing the middle and not touching each other. Each sandwich could be transferred safely into and out of the stack in the round NMR sample tube without scratching the films and thereby damaging them. Opening the sandwich was important, because after 4 or 5 days of experiments the sample had to be rehydrated and this proved to be most efficient when the entire film was exposed (see below).

Trapping the M State and Light Adaptation. Illumination of the GuaHCl-treated films of wild-type bR with yellow light showed that the M decay at room temperature was slowed down to a few seconds, the same as for the D96A containing films. The lifetime was observed to further increase by a factor of about 10 at 5 °C. Since the material on each plate had a high optical density, it was necessary for the plates to be bleached individually in order to bring them into the M state. Thus, after hydration for 12 h or more at room temperature, the plates were taken out of the box and brought to a cold room at 5 °C. After being cooled and equilibrated for about 20 min, they were illuminated with yellow light (550 nm band-pass filter) from the fiber bundle of a 150 W cold light source (FOSTEC, New York) causing the purple films to bleach to a bright yellow. A pair of plates was then assembled as a sandwich in the yellow light and transferred to the 30 mm long NMR sample tube having a

10 mm diameter which was lying on dry ice. During the transfer, the sandwich was illuminated with another fiber bundle to keep the sample in the M state. Our aim was to generate the M state at temperatures above freezing to ensure that the fully functional intermediate was trapped. The freshly inserted sandwich was allowed to equilibrate for at least 1 min before the next one was transferred. Heat exchange between the cold and newly transferred plate ensured that the latter froze quickly. After all plates were inserted, the tube was closed with a plug and kept in the dry ice box.

The strategy of light adaptation made use of the fact that bR molecules which return thermally from the M state have an *all-trans* chromophore. Thus, the plates were illuminated at room temperature with yellow light as described above, until they were brightly yellow without any purple traces. They became purple after the yellow light was removed. In addition, they were exposed to blue light which induces a back-photoreaction from M to bR_{all-t} (*35*), which also leads to an *all-trans* chromophore. Finally, the sandwich was inserted into the sample tube lying on dry ice as described above. The time for transfer from the yellow light to the blue light and into the sample tube was less than 45 s, and thus no 13-*cis* chromophore could have formed (*30*). The long lifetime of M at room temperature allowed one to make sure that the entire sample was yellow in the first step and consequently that it was 100% light adapted after thermal relaxation and blue light illumination.

The closed box with the sample tube on dry ice was then taken to the NMR magnet where the probe head had been precooled to −50 °C for several hours. Within about 1 min the probe head was taken out of the magnet, the sample tube inserted in the horizontal solenoid, and the probe head put back into the magnet. This time is critical, because during this procedure the probe head must be disconnected from the cold nitrogen supply and starts to heat up. Most importantly, after each experiment of 4−5 days duration, the sample tube was removed quickly from the cold probe head and put on dry ice. The sandwiches were then taken out and checked for color. If the plates were no longer yellow, but appeared to be darker or even of purple color, the experimental data were discarded. This occurred only once. After rehydration, the plates could be bleached again without problems. Thus, they were cycled for up to ten times and remained functional.

^{2}H NMR Spectroscopy. ^{2}H NMR experiments were performed with a 7.05 T wide-bore magnet and a Bruker AMX300 console. The probe head with a 20 mm long and 10 mm diameter horizontal solenoid was home built and cooled to −50 °C by a flow of nitrogen directed at the coil. The deuterium signal at 46.13 MHz was recorded using a quadrupolar echo sequence ($90^\circ_x - \tau - 90^\circ_y - \tau -$ acquire) with a 90° pulse length of 3.1 μs at 1 kW power from a Henry radio amplifier and a standard eight-step phase cycle. The delay times $\tau \simeq 42$ μs were determined with a powder sample of perdeuterated plexiglass. The recycle time of 200 ms did not seem to result in any appreciable saturation of the signal. The echo was digitized using 4096 points with a dwell time of 0.5 μs. In one continuous experiment, 400 000 echoes were recorded over 24 h. An exponential multiplication of 2 kHz was applied to the echo decay before Fourier transformation. Between two and eight such spectra were subsequently added to improve the signal-to-noise figure, if no systematic differences appeared to exist between the individual sets.

^{2}H NMR Line-Shape Analysis. The procedure of numerically analyzing the ^{2}H NMR line shapes is described in detail elsewhere (*18*). In short, because the quadrupolar interaction depends on the angle θ between the magnetic field and the deuterated bond, only one pair of lines is expected for a sample in which all bonds make the same angle θ with the magnetic field (for a review see ref *36*). Their frequency separation (quadrupolar splitting) is given by

$$\Delta\nu_Q = \Delta\nu_Q^{powder}(3\cos^2\theta - 1) \qquad (1)$$

where $\Delta\nu_Q^{powder}$ depends on the quadrupolar coupling constant and equals the splitting of the two lines for $\theta = 90°$. It has a value of approximately 40 kHz for a methyl group in the fast motional limit which applies to our samples (*37*). Since neither the sign of $\Delta\nu_Q$ nor the sign of $\Delta\nu_Q^{powder}$ can be determined experimentally, two solutions are possible for a splitting $|\Delta\nu_Q| \leq |\Delta\nu_Q^{powder}|$. In the case of a (perfectly) uniaxially aligned membrane sample all bonds lie on the rim of a cone around the orientation axis whose half-angle is the angle between the bond and the membrane normal. At 0° tilt, i.e., when the orientation axis and the magnetic field are parallel, the angle θ corresponds to the angle between the bond and the membrane normal and can be directly determined from the splitting of the two observed lines. At a different sample tilt, however, the distribution of bonds around the magnetic field is characteristic for the cone angle and allows one to distinguish the two solutions of eq 1 (*18*, *38*).

The experimental quadrupolar line shape reflects the probability density of all bond orientations in the sample. Usually the sample is not perfectly uniaxially oriented, i.e., the individual membrane normals are not perfectly aligned but are distributed around the glass plate normal, and the line shape consists of inhomogeneously broadened lines. This distribution is known as the mosaic spread of the sample. In this case, an assumption must be made about the shape of the distribution in order to determine the bond orientation with respect to the membrane normal from the ^{2}H NMR line shape. The Monte Carlo procedure for simulating the line shape allows any arbitrary distribution to be included (*18*, *39*). Whereas in previous publications a Gaussian distribution was found to be sufficient to simulate the ^{2}H NMR spectra (*18*, *38*), this was not so with the present samples. We therefore tried several other forms of disorder and obtained the best results with either a Lorentzian distribution or a sum of two Gaussian distributions having an adjustable weighting factor and half-width ratio.

The quality of the line-shape simulation was determined from the residuals, and a simulation was considered acceptable if no significant deviations from the apparent noise could be detected. Since the simulation has five adjustable parameters, viz., the coupling constant $\Delta\nu_Q^{powder}$, the intrinsic line width, the width of the mosaic spread, the sample tilt, and the bond orientation, it is essential to use as many experimental data as are available in order to restrict the range of values as much as possible. Previously (*18*), we have independently determined the coupling constant and intrinsic line width from a powder-type sample and a T_2 relaxa-

tion experiment, respectively. Thus, the coupling constant $\Delta\nu_Q^{powder}$ was varied only within the interval 39 ± 1 kHz and the intrinsic linewidth (FWHM of a Lorentzian) within 3.5 ± 0.5 kHz. In a powder-type sample or in the presence of large mosaic spread, $\Delta\nu_Q^{powder}$ determines essentially the separation of the two prominent horns in the spectra (see Results) and therefore shows little correlation with the other parameters. An increase in mosaic spread changes mainly the height of these horns in the line shape relative to the shoulders, as the distribution of membrane normals becomes wider and the line shape becomes reminiscent of that of a powder-type sample (see Results). Consequently, the mosaic spread is also only weakly correlated with the other parameters. It was characterized either by its Lorentzian half-width or, in the case of two Gaussians, by their half-widths and their integral ratio. The sample tilt angle was varied within ±3° around the set angle to accommodate for imperfect adjustment. It has only a minor effect on the line shape. In the presence of substantial mosaic spread, the bond orientation cannot be read off the line shape directly, and varying its value affects the line shape in many ways. In our experiments, where the bond orientations are rather close to the magic angle, this parameter largely determines the intensity in the middle of the spectrum around the carrier frequency, because the corresponding splitting is relatively small. Since the other parameters are very well defined, the uncertainty of the bond orientation in the simulation of a single spectrum is less than 5°; i.e., choosing a value more than 5° away from the optimal value increases the residuals substantially. In order to increase the precision, all data sets measured for an individual sample, including dark-adapted, light-adapted, and M state spectra at all tilt angles, were simulated at the same time. In this way, parameters common to all of them, i.e., the coupling constant, intrinsic line width, and mosaic spread, are even better defined. Moreover, the bond orientation is independent of the tilt angle, and consequently, the entire tilt series in one state of the sample must be fitted with the same value for this parameter, again increasing the precision with which this value is obtained. As a result, the uncertainty in the determination of the bond orientation from all spectra taken together is not larger than 3°. In all the figures, the spectra are scaled such that they have the same integral.

RESULTS

^{2}H NMR Line Shapes. A set of representative ^{2}H NMR line shapes, recorded at 0° sample tilt, is shown in Figure 2 for the wild-type sample with a C_9-CD_3 deuterated methyl group. The figure illustrates the changes in the line shapes for several preparations: the dark-adapted sample, the light-adapted sample, and two M preparations. The spectrum labeled M (50%) state is from an experiment at the end of which the films were no longer completely yellow, but of an intermediate darker color, and thus no longer entirely in M. Superimposed on each spectrum in the figure is the spectrum of the light-adapted sample (gray lines). Below each spectrum in Figure 2, the difference with respect to the light-adapted sample is indicated. Almost no systematic deviation from the noise is observed for the dark-adapted state (spectrum labeled "dark adapted" of Figure 2), but very clear differences are discernible for the M state experiments. The differences are positive near the spectral center (carrier or

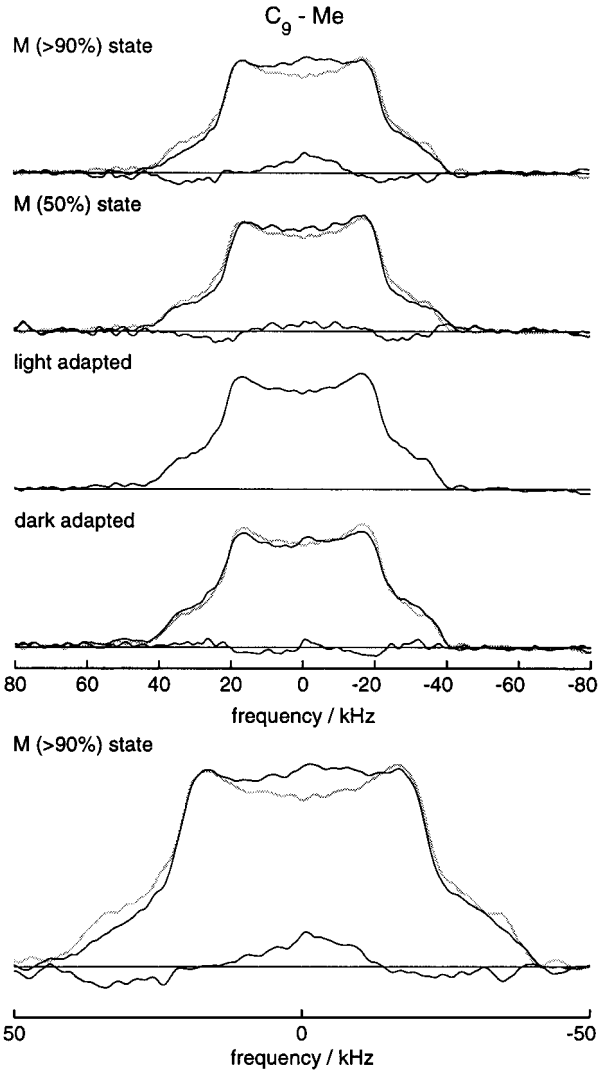

FIGURE 2: ^{2}H NMR spectra from wild-type bacteriorhodopsin regenerated with C_9-CD_3-labeled retinal and treated with a guanidine hydrochloride solution. In each case the membrane normal is parallel to the magnetic field (zero sample tilt). Data at −50 °C are shown for the dark- and light-adapted state and two different M experiments. In the M spectrum labeled 50%, the films were no longer completely yellow at the end of the experiment as was the case with the top spectrum (>90%). Superposed on each spectrum (—) is the light-adapted spectrum (gray line) and below it the difference between the two. Each spectrum consists of about 1.6 million acquisitions collected over 4 days. In the bottom part, the M spectrum (>90%) is enlarged. For a detailed discussion see text.

Larmor frequency) and negative in the shoulder region of the M state spectra and are more pronounced the more M is formed (compare the spectra labeled 50% and >90%). One can thus conclude that the bond orientation changes in the transition from the ground state to the M state. The C_9- methyl group is known to make an angle of about 40° with respect to the membrane normal in the ground state (*17*). Since the intensity shifts toward the carrier frequency (0 kHz) in the M state (positive difference in the middle), we conclude from eq 1 that only an increase of the angle between bond and magnetic field to more than 40° can cause a smaller quadrupolar splitting in the M state. To determine the bond angles numerically, a detailed analysis of the line shapes is required.

In previous publications (*17*, *18*), the ^{2}H NMR spectra at 0° sample tilt consisted of two broad lines whose splitting

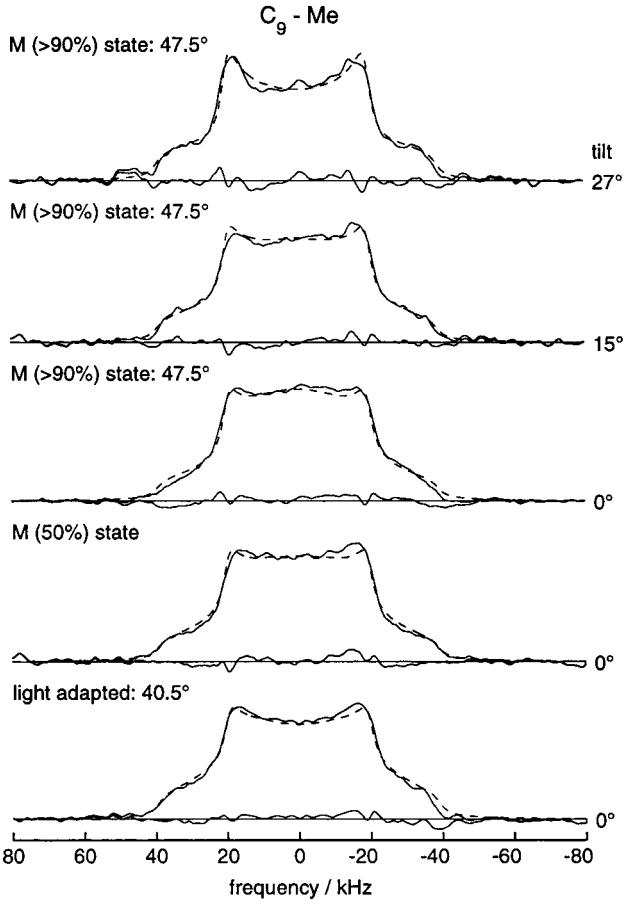

FIGURE 3: ^{2}H NMR spectra at −50 °C (—), their line-shape simulations (- - -) and residuals (—) for the C_9-CD_3-labeled wild-type bacteriorhodopsin sample of Figure 2. The angle for the bond orientation is 40.5° in bR_{all-t} and 47.5° in M. The sample tilt angles are indicated to the right of each spectrum. The other fit parameters are $\Delta\nu_Q^{powder}$ = 39.2 kHz, line broadening 3.9 kHz (Lorentzian FWHM), and a mosaic spread of 27° (Lorentzian FWHM). The simulated spectra are corrected for the finite pulse length (*50*).

corresponded approximately to the average angle θ according to eq 1 (cf. bottom spectrum of Figure 5). The samples used in those studies were not exposed to the GuaHCl treatment required in this work, which leads to a decrease in the orientational order of the membranes in the films. In Figure 2, the two horns have the same separation, viz., ca. 40 kHz, for all spectra. It depends neither on the state of the protein (dark adapted, light adapted, or M) nor on the tilt angle (cf. Figure 3). The explanation for this difference in the line shapes lies in a significantly larger mosaic spread (disorder) than in the previous experiments. In the case of an isotropic distribution of bond angles (powder-type sample), the resulting Pake pattern of the line shape also displays two prominent horns separated by $\Delta\nu_Q^{powder}$ and shoulders at each side of the spectrum, reminiscent of the line shapes in Figure 2. The horns of the Pake pattern are due to the fact that the polar angles θ are weighted with sin θ leading to the integrable singularities at $\theta = 90°$. For a powder-type sample, however, the line shapes are independent of the bond orientation with respect to the membrane normal and also independent of the sample tilt. This is clearly not the case here, because there are systematic differences between the light-adapted and M state spectra (Figure 2), as well as the M state spectra at various tilt angles (Figure 3). The former are due to a change in bond orientation, because the mosaic spread is the same for the ground and M states, and the latter are caused by a change in the distribution of θ, when the sample is tilted. From the fact that the separation of the horns in our spectra is independent of the sample state and inclination, we conclude that there are always some bonds, which are oriented at right angles with respect to the magnetic field. This is due to the large mosaic spread. On the other hand, the samples are not isotropically disordered, because the line shapes as a whole do exhibit differences depending on the protein state or plate tilt. Still, the bond angle with respect to the membrane normal cannot be read off from the main peak separation in the spectra at 0° sample tilt, as was possible in previous work (*17*, *18*). The reason is that rehydration of the oriented membrane films with a concentrated solution of GuaHCl, necessary to prolong the M lifetime, leads to an appreciable increase in the mosaic spread. A numerical simulation of the line shape is thus essential and does not merely represent a refinement of the directly determined value.

An important element of this simulation is the distribution of membrane normals with respect to the glass plate normal (mosaic spread). In previous experiments on the ground state of bR, a Gaussian distribution was shown to be adequate (*17*, *18*). For the line shapes in Figures 2 and 3 this proved to be insufficient for an acceptable simulation, mainly because the shoulders were not reproduced unless the Gaussian half-width was increased to $\sigma \geq 35°$, but even then the fit of the experimental data was poor. Instead, either a superposition of two Gaussian distributions with a half-width ratio of about 4 or a Lorentzian distribution gave good results. In both cases, the feet of the distribution are wider with respect to the central part than for a single Gaussian. A Lorentzian mosaic spread can, as an approximation, be interpreted as representing a continuum of Gaussian distributions with increasing half-widths. Such a superposition may in fact be expected, because the films are not entirely homogeneous, and the stacking order of the purple membranes will vary from the upper layers (largest disorder) to the bottom layers near the glass surface. This is especially true in the case of the GuaHCl-treated films. It should be noted that, strictly speaking, the mosaic spread determined from ^{2}H NMR need not be identical to that found in diffraction experiments. The reason for this is that in ^{2}H NMR the spectral line shape is a linear sum of the contributions from all deuterium atoms in the sample, whereas in crystallography periodicity of the unit cell arrangement is a prerequisite and only those portions contribute which are ordered in a lattice. The diffracted intensity then depends quadratically on the number of unit cells in a two-dimensional lattice. Therefore, if the disorder in the sample is caused by the breaking up of periodic arrays of unit cells, the mosaic spread measured with the two methods will be different.

C_9-CD_3 Labeled Retinal. As described above, oriented films of wild-type bR regenerated with C_9-CD_3-labeled retinal were treated with GuaHCl to prolong the lifetime of M. Figure 2 shows the ^{2}H NMR spectra and their differences versus the data measured with the light-adapted sample. These differences were discussed qualitatively above. The simulations (- - -) of the line shapes in Figure 3 show that in each case a very good fit was achieved with only randomly fluctuating residuals. Moreover, the simulations confirm our

interpretation that the C_9-CD_3 bond angle with respect to the membrane normal is greater in the M state than in the ground state. It increases from 40.5° in the light-adapted ground state to 47.5° in the M state. Also, the tilt angle dependence of the ^2H NMR line shape in the M state is reproduced very well (Figure 3) and proves that the sample is not isotropically disordered. The best fits were achieved with a Lorentzian distribution for the mosaic spread with a FWHM = 27°. In comparison, the hydrated films not treated with GuaHCl used in earlier experiments (*17*, *18*) showed a Gaussian distributed mosaic spread with a FWHM of about 19° ($\sigma \simeq 8°$). Due to the relatively large degree of disorder of the GuaHCl-treated films, the line shapes are not as sensitive to the bond angle as in untreated samples. However, the error for the difference between the ground and M state values is not directly related to this insensitivity, because an increase of the bond angle, for example, can be distinguished without ambiguity from a decrease. We have varied the bond angle values for simulations with the same mosaic spread, coupling constant $\Delta\nu_Q^{powder}$, and intrinsic line broadening and have determined the quality of the fits by inspecting the residuals. We find that the values of the angles are undetermined within a ±3° interval, but the error for the difference between the ground and M state values is not larger, and possibly smaller, because the sign of the change in angle can be determined unambiguously from the line shape (see below).

The ground state value for the C_9-CD_3 bond orientation of 40.5° is in excellent agreement with an earlier value of 40° determined with a better oriented sample not treated with GuaHCl (*17*). This shows that the addition of GuaHCl does not affect the bond orientation. More importantly, it proves that the line-shape simulation allows one to extract the correct angle even in the presence of a large mosaic spread. The simulation of the ^2H NMR spectra measured at three tilt angles demonstrates that the angle in M is not the alternative solution of eq 1 (ca. 63°), but indeed the smaller one of 47.5°, because the line shapes are clearly different for the two solutions despite the large mosaic spread (simulations not shown) (*18*, *38*). Also, the simultaneous line-shape simulation of all five spectra in Figure 3 with a fixed common set of parameters except the bond angle increases the precision with which the bond orientation is determined. In earlier work (*25*), the angle for the C_9-CD_3 bond orientation in the M state was reported to be 44 ± 2°, but due to the fact that the probe head had to be brought to room temperature before the sample could be inspected, these authors were unable to prove that their sample was still in the M state after completion of the experiments. As described in Materials and Methods, we have quickly removed the sample from the cold probe head after completing the data acquisition and have confirmed for all experiments that the films were still yellow. The results of one experiment, at the end of which the sample had a darker color, are included in Figures 2 and 3 (labeled 50% M). Its line shape was simulated by a superposition of the pure ground and M state spectra (with bond angles of 40.5° and 47.5°, respectively), and only the ratio of the two was varied. The best mixture was found to be about 1:1, in good agreement with the visual impression. The importance of the visual control at the end of the experiment cannot be overemphasized. Compared to the previous experiments (*25*) our signal-to-noise ratio is much improved. Moreover, we did not symmetrize the spectra as was done in ref *25*, because this may lead to severe distortions especially in noisy spectra.

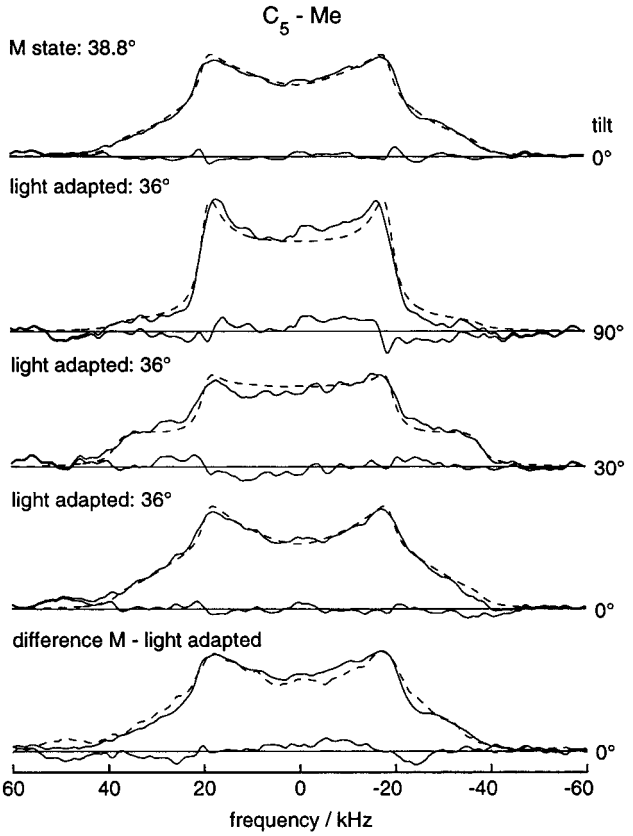

FIGURE 4: ^2H NMR spectra at −50 °C (—) with simulation (- - -) and residuals for the C_5-CD_3-labeled D96A sample (upper four spectra). In the bottom spectrum, the difference between the M state (—) and the light-adapted spectrum (- - -) demonstrates the existence of a systematic change in the line shape having features similar to those observed for the C_9-CD_3 group (Figure 2). The angle for the C_5-CD_3 bond orientation obtained from the numerical analysis of the upper four spectra is 36° in bR_{all-t} and 38.8° in M. The sample tilt angles are given to the right of each spectrum. The fit parameters are $\Delta\nu_Q^{powder}$ = 38.2 kHz, line broadening 3.7 kHz (Lorentzian FWHM), and a mosaic spread with two Gaussian distributions of width σ 9.4° and 42.3°, respectively, and an integral ratio of 2:1. The simulated spectra are corrected for the finite pulse length (*50*).

C_5-CD_3 Labeled Retinal. In this case, purple membranes containing the D96A mutant of bR were regenerated with the C_5-CD_3 deuterated retinal. The signal from this sample (Figure 4) was weaker than those from the other samples, and the spectra consequently are noisier. At the bottom of Figure 4, the difference between the ground and M state spectra shows the same signature as in the case of the C_9-CD_3 bond: a small positive difference in the middle of the spectrum and a negative one in the shoulder region. The simulations confirm the small increase of the bond angle from 36° in bR_{all-t} to 38.8° in M. This difference is close to the error of 3° given above for the absolute angles. On the other hand, the difference in the data unambiguously demonstrates that the bond tilts away from the membrane normal, i.e., that the angle increases. Thus, it may be concluded that the error for the change in angle is clearly less than 3°. In the case of the mutant protein, the mosaic spread described by two superposed Gaussian distributions gives better results

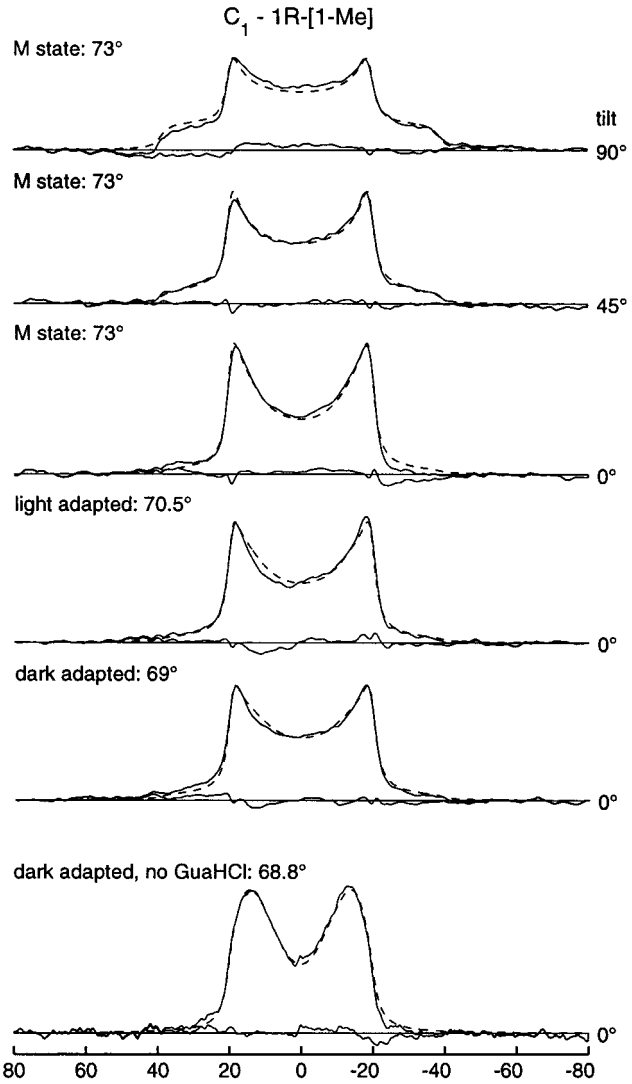

FIGURE 5: ^{2}H NMR spectra at −50 °C (—) from the 1*R*-[1-CD_3]-labeled wild-type sample of bacteriorhodopsin treated with GuaHCl together with their line-shape simulations (- - -) and residuals. The bottom spectrum was recorded at −50 °C before the film was treated with GuaHCl. After the GuaHCl solution was applied, the mosaic spread increased substantially (upper five spectra). The angle for the bond orientation is 69° in the dark-adapted mixture of bR_{13-c} and bR_{all-t}, 70.5° for bR_{all-t}, and 73° in M. The sample tilt angles are indicated to the right of each spectrum. The values of the fit parameters are $\Delta\nu_Q^{powder}$ = 39.05 kHz, line broadening 3.2 kHz (Lorentzian FWHM), and a mosaic spread of 24° (Lorentzian FWHM). The simulated spectra are corrected for the finite pulse length (*50*).

than a Lorentzian distribution, although the improvement is only marginal. This could be interpreted as being indicative of different purple membrane populations in the sample.

1R-[1-CD_3]-Labeled Retinal. In a previous study, we investigated bR containing retinal stereospecifically labeled in one of the two geminal methyl groups on carbon C_1 of the cyclohexene ring in the absence of GuaHCl (*18*). Figure 5 illustrates how much the line shape at 0° sample tilt changes due to the GuaHCl-induced increase in mosaic spread. The bottom spectrum of Figure 5 shows the line shape at 0° sample tilt before the GuaHCl solution was applied to the films. After the treatment, the line shape is very different, although conditions are otherwise identical (Figure 5, spectrum labeled "dark adapted: 69°"). This clearly demonstrates how the quality of orientational order suffers from the application of the GuaHCl solution, which results in a swelling of the films particularly near the surface. Whereas the bond angle could be read off fairly accurately from the 0° tilt spectrum before the GuaHCl treatment (the peak separation of ca. 26 kHz corresponds to a bond angle of either 42° or 71°, depending on the sign of the splitting), this is impossible for the ^{2}H NMR spectra of bR treated with GuaHCl in Figure 5. Due to the increased mosaic spread, the prominent horns now correspond to the 90° orientation of the bond with respect to the magnetic field. However, the bond orientation determined from the line-shape simulation for the dark-adapted state in the presence of GuaHCl (69°) agrees very well with our previous results of 68.8° at 20 °C and 68.6° at −50 °C in the absence of GuaHCl (*18*). This illustrates, again, the importance and reliability of the line-shape simulations. Interestingly, only in this sample was a slight difference of the bond orientation in the light- and dark-adapted states observed (second and third spectra from the bottom in Figure 5), viz., 69° in the dark-adapted mixture of bR_{13-c} and bR_{all-t} and 70.5° in bR_{all-t}. This may indicate a change in the angle of the ring plane rather than a change in the chain tilt, because the 1*R*-[1-CD_3] bond is more sensitive to the plane tilt than a rotation around the ring plane normal. Between bR_{all-t} and the M state, the change amounts to 2.5°, i.e., from 70.5° to 73° in M. Again, the tilt series demonstrates that the bond orientation is 73° and not the smaller angle solution of eq 1.

DISCUSSION

The retinylidene chromophore of bacteriorhodopsin constitutes the antenna for the energy input, and its Schiff base serves as the proton source of this light-driven ion transporter. The M intermediate plays a key role in the photocycle, because the first major charge translocation is associated with its formation. During the lifetime of the M state, the proton accessibility of the Schiff base changes presumably from the extracellular to the cytoplasmic side, and this switch is essential for the vectoriality of transport (*40*). In the present work, the chromophore orientation with respect to the membrane normal was investigated with deuterium solid-state NMR. Three differently ^{2}H-labeled retinals were incorporated into wild-type bR or the D96A mutant. The M intermediate as well as the light-adapted ground state were cryotrapped, and the angle between the three methyl bonds C_9-CD_3, C_5-CD_3, and 1*R*-[1-CD_3] (see Figure 1) and the membrane normal were measured in the two states. In a previous study, we showed that experiments performed at −50 °C, i.e., the condition necessary to trap the M state for the duration of an NMR experiment, give the same results as those performed at room temperature (*18*). Apparently, freezing does not change the chromophore structure in the binding pocket, which is only an assumption in the case of electron cryomicroscopy. At the same time, great care was taken to generate the M state above 0 °C, because the mobility of water molecules may play a role in its formation. Only after the sample was brought into the M form did we lower the temperature. Thus, the results of the present study are relevant for elucidating the pumping mechanism and understanding the cofactor−protein interaction. As discussed in the introduction, under the conditions of our experiments the M intermediate was most likely trapped in a substate in which the major protein conformational change has occurred.

A thorough numerical analysis of the ^{2}H NMR line shapes was required to determine the angle of the deuterated methyl bond with respect to the membrane normal. The values in the dark-adapted ground state are in excellent agreement with previously published results (*17*, *18*) for all three methyl groups investigated. In ref *17* values of 40° for the C_9-CD_3 bond and 37° for the C_5-CD_3 bond were obtained compared to 40.5° and 36°, respectively, in the present study. In the case of the 1*R*-[1-CD_3] bond, we have previously reported (*18*) a value of 68.7°, identical to the 69° value measured here for the GuaHCl-treated sample. This excellent agreement proves that our line-shape analysis is reliable even in the presence of considerable mosaic spread. In addition, these results show convincingly that the GuaHCl treatment does not affect the chromophore orientation.

Only with the 1*R*-[1-CD_3]-labeled retinal did we find any difference between the dark-adapted bR preparation, which contains a mixture of *all-trans* and 13-*cis* chromophores, and the purely *all-trans* light-adapted state bR_{all-t}. The difference is minor (1.5°) and may mainly reflect a change in the ring plane tilt. The angles in the M state differ much more from the corresponding values for bR_{all-t}. The largest difference is seen in the C_9-CD_3 position, where the bond orientation changes by 7°. The C_5-CD_3 bond changes by only 2.8° and the 1*R*-[1-CD_3] bond by 2.5°. All angles with respect to the membrane normal increase compared to the ground state. Since the plane of the conjugated system is nearly perpendicular to the membrane surface within 30°, both in the initial state and in M (*19*, *41*), the changes of the methyl bond orientations on the polyene chain may be explained by a tilt of the retinal around the normal to the cyclohexene ring plane. If the conjugated system were planar and not twisted, the different changes in the C_5-CD_3 and C_9-CD_3 orientations would indicate a different bending of the chain in the M state compared to the ground state. On the other hand, torsional strain and twists of the polyene chain may also be an explanation for the changes in bond orientation.

Comparison with Results from Other Methods. Our results on the change in orientation of the C_1-, C_5-, and C_9-methyl bonds in M are unique, and no comparable information has been obtained by any other structural method. ^{2}H NMR with oriented proteins containing specifically deuterated cofactors is clearly able to provide valuable and accurate local structural information.

On the basis of the reorientation of the two methyl groups of the β-ionone ring and a simplified, planar geometry of the retinal, we calculate that in M the C_5-N vector tilts into the plane of the membrane by about 5° as shown in Figure 6 (for the method see ref *18*). This reorientation of the polyene chain may be compared with results from neutron diffraction and polarized absorption spectroscopy.

Neutron diffraction experiments with specifically deuterated retinals have demonstrated that, in the projection onto the membrane plane, the position of the cyclohexene ring does not change from bR_{all-t} to M but that the Schiff base end moves 1.4 ± 0.9 Å toward the ring (*22*). The authors concluded that the C_5-C_{13} vector tilts away from the membrane plane by 11 ± 6° (*22*). Assuming that the conjugated system is planar, the angle between the C_5-N and the C_5-C_{13} vector in the 13-*cis* form is about 9.5°. This assumption of a planar chain is supported by polarized FTIR (*19*) and polarized resonance Raman experiments (*41*), which also show that the polyene plain is almost perpendicular to the membrane plane. Subtracting 9.5° from the 5° change of the C_5-N orientation found in our calculations leads to the conclusion that the C_5-C_{13} segment moves out of the membrane plane by 4−5°, in reasonable agreement with the neutron diffraction data. Figure 6 illustrates the proposed structural change in M.

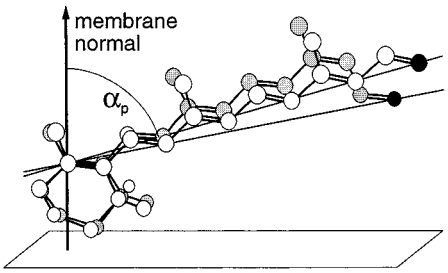

FIGURE 6: Retinal orientation in the light-adapted (*all-trans*, white atoms) and the M state (13-*cis*, shaded atoms) of bacteriorhodopsin obtained from ^{2}H NMR constraints for the C_5-CD_3 and 1*R*-[1-CD_3] bonds. The retinal structure is based on the geometry of sp^2 and sp^3 hybridized orbitals. The C_5 carbon and the Schiff base nitrogen are connected by a line in each state. The C_5-N vector characterizes the molecular long axis and is close to the optical transition dipole moment in the *all-trans* conformer. Its inclination with respect to the membrane normal is designated by the angle α_p and has a value of 74° in the ground state and 79° in the M intermediate. Note that this change is largely due to the isomerization. In this figure, the C_5 atom was assumed to have the same coordinates in both states.

Results from linear dichroism spectroscopy indicate that the chromophore transition dipole moment changes its direction with respect to the membrane normal in M by only a very small amount (*23*, *24*, *42*, *43*). The most sensitive measurements find that the transition dipole moment orientation tilts out of the membrane plane by 2−3° (*23*, *24*, *42*). Whereas the transition dipole moment coincides in a good approximation with the C_5-N vector of *all-trans* retinal (*44*), similar information is not available for the M state 13-*cis* chromophore with a deprotonated Schiff base. Since it is not known how the M transition dipole moment is fixed in the chromophore molecular frame, a meaningful comparison with the NMR results is not possible.

In a planar, linear polyene chain, the molecular axis C_5-C_{13} tilts uniformly, and the change in bond orientation is the same for the C_5-CD_3 and C_9-CD_3 groups. Experimentally, the orientation change at position C_9 is 4° larger than at C_5. Thus, it is reasonable to hypothesize that the C_9-CD_3 group interacts sterically with the protein and is bent with respect to the polyene chain or that the polyene chain from C_5 to C_{13} does not simply tilt upon isomerization but becomes bent or twisted in a different way than in the ground state. The transition dipole moment may be tilted away from the membrane plane as a consequence. The upward movement of the C_5-C_9 ($-C_{13}$) chain segment after photoexcitation may cause structural changes in the protein which eventually lead to deprotonation of the Schiff base. In the absence of such interactions between retinal and the protein, even the 13-*cis* conformer retains its protonated Schiff base.

Linear dichroism has also been used to detect possible changes of the transition dipole moment in light−dark adaptation. In this case, no deprotonation of the Schiff base occurs, and it seems reasonable to assume that in both isomers the transition dipole moment has approximately the

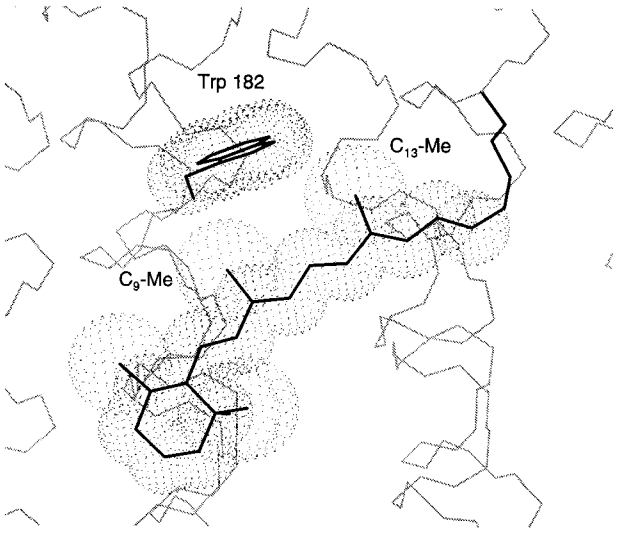

FIGURE 7: Side view of the retinylidene chromophore of bacteriorhodopsin in its binding pocket. The atomic coordinates were taken from the ground state structure determined with electron cryomicroscopy (*12*). The backbone is shown in gray. The structure of the chromophore, lysine 216, as well as tryptophan 182 are drawn in black, and the van der Waals spheres around the carbon atoms are indicated. The spheres around the methyl group carbons are increased in order to take into account the missing hydrogen atoms. Note that the C_9−methyl group is in close proximity to the indole ring of tryptophan 182 and may interact with it sterically when the polyene chain moves up in M after the *all-trans* to 13-*cis* isomerization.

direction of the C_5−N vector (*44*). No significant differences were observed in the linear dichroism spectra of light- and dark-adapted oriented purple membranes (*24*, *45*), indicating that no change in transition dipole moment orientation with respect to the orientational axis occurs. These results are consistent with our ^{2}H NMR experiments, in which no significant reorientations of individual methyl bonds were detected.

Possible Interaction of the Chromophore C_9−Methyl Group with W182 in M. The relatively large angular change of the C_9−CD_3 bond may be due to torsional strain or to an orientational change of the C_5−C_{13} portion of the polyene chain toward the cytoplasmic side of the membrane. In either case, changes in steric contacts with the binding pocket are expected, and these could serve as the steric trigger for structural changes in the protein. In the dark-adapted state of bR, the planar indole ring of tryptophan 182 is in close proximity to and just above the C_9−methyl group (*12*, *13*), as shown in Figure 7. According to the latest three-dimensional X-ray structure, the distance between the C_9−methyl group and the indole nitrogen of tryptophan 182 in the dark is only 3.9 Å (*46*). Upward movement of this methyl group in M will thus be obstructed by the indole group, and this steric interaction may lead to the observed tilt of helix F to which W182 is attached (*16*). Proline 186 was suggested to act as the hinge for this outward movement of the cytoplasmic half of helix F in M (*16*). This suggestion was supported by the very high temperature factors for the backbone of helix F between the kink at P186 and the cytoplasmic surface (*12*). Since tryptophan 182 is located between the putative hinge position and the cytoplasmic loop domain, it is indeed in an appropriate position to serve in the coupling between chromophore and helix movement. Strong indirect evidence for a steric interaction between the C_9−methyl group and W182 in the course of the photocycle was obtained from FTIR and flash spectroscopy measurements with tryptophan mutants and with the 9-desmethyl retinal analogue (*9*−*11*). Removal of the C_9−methyl group or replacement of the bulky indole side chain of tryptophan 182 by phenylalanine had the same effect, and both led to a drastic increase in the lifetime of the N intermediate (250-fold). A steric interaction between the C_9−methyl group and W182 seems to be essential for the 13-*cis* to *all-trans* reisomerization of the chromophore (*10*). Whereas all previous experiments suggesting such an interaction (*9*−*11*, *13*) used spectroscopic methods in conjunction with mutants and retinal analogues, our result of a 7° increase in orientation of the C_9−CD_3 bond in M was obtained with wild type and provides direct structural evidence for movement of this methyl group toward W182. In the related retinal protein rhodopsin, the C_9−methyl group also plays a crucial functional role in the coupling between the cofactor and apoprotein. It provides the structural anchor for the correct docking of the chromophore in its binding site (*47*). Steric interaction of this methyl group with helix C in the vicinity of glycine 121 seems essential for activation (*48*), and removal of this methyl group leads to a strong reduction of transducin activation (*49*).

The changed interaction of the chromophore with its binding pocket after isomerization drives the inactive retinal protein into an activated state (M state of bR or metarhodopsin II) in which proton transport or molecular recognition by a G protein in the case of rhodopsin can occur. Not only do the two moieties mutually influence their physical properties, e.g., the opsin shift in the absorption spectrum of retinal bound to bR or rhodopsin, but their steric interaction triggers and controls protein function. In the future, it will be interesting to determine the orientation of individual chromophore methyl bonds in earlier intermediates of the photocycle of bR, because it is not yet clear what constitutes the molecular basis of the switch in bR, where the proton accessibility of the Schiff base changes from the extracellular to the cytoplasmic side (*40*).

Although ground state structures determined by crystallographic methods offer valuable insights and can inspire new ideas (*12*, *46*), only with knowledge of the structural properties of intermediate states can a complete understanding of the intricacies of macromolecular function be achieved. In this respect, the ^{2}H NMR method used in this study offers considerable promise. It focuses on the local orientational change of the specifically deuterated cofactor. In many systems, the cofactors can be exchanged by deuterated analogues. In photoreceptors such as rhodopsin, phytochrome, or the photoactive yellow protein, light-induced isomerization of the chromophoric cofactors occurs with associated chromophore reorientation. Moreover, the cofactors are often the sites of enzymatic action and therefore of particular interest. Using this isomorphic labeling strategy, orientational changes of individual methyl bonds may be detected with high accuracy in the trapped intermediates of the functional cycle.

ACKNOWLEDGMENT

We are greatly indebted to Constantin Job for outstanding support in all technical aspects of the NMR experiments. Alexander Nevzorov not only provided valuable mathemati-

cal insight, but also contributed to a congenial working environment.

REFERENCES

1. Mathies, R. A., Lin, S. W., Ames, J. B., and Pollard, W. T. (1991) *Ann. Rev. Biophys. Biophys. Chem. 20*, 491−518.
2. Harbison, G. S., Smith, S. O., Pardoen, J. A., Winkel, C., Lugtenburg, J., Herzfeld, J., Mathies, R. A., and Griffin, R. G. (1984) *Proc. Natl. Acad. Sci. U.S.A. 81*, 1706−1709.
3. Smith, S. O., Courtin, J., van den Berg, E., Winkel, C., Lugtenburg, J., Herzfeld, J., and Griffin, R. G. (1989) *Biochemistry 28*, 237−243.
4. Fodor, S. P., Pollard, W. T., Gebhard, R., van den Berg, E. M., Lugtenburg, J., and Mathies, R. A. (1988) *Proc. Natl. Acad. Sci. U.S.A. 85*, 2156−2160.
5. Hu, J. G., Sun, B. Q., Petkova, A. T., Griffin, R. G., and Herzfeld, J. (1997) *Biochemistry 36*, 9316−9322.
6. Ames, J. B., Fodor, S. P., Gebhard, R., Raap, J., van den Berg, E. M., Lugtenburg, J., and Mathies, R. A. (1989) *Biochemistry 28*, 3681−3687.
7. Farrar, M. R., Lakshmi, K. V., Smith, S. O., Brown, R. S., Raap, J., Lugtenburg, J., Griffin, R. G., and Herzfeld, J. (1993) *Biophys. J. 65*, 310−315.
8. Fodor, S. P., Ames, J. B., Gebhard, R., van den Berg, E. M., Stoeckenius, W., Lugtenburg, J., and Mathies, R. A. (1988) *Biochemistry 27*, 7097−7101.
9. Weidlich, O., Friedman, N., Sheves, M., and Siebert, F. (1995) *Biochemistry 34*, 13502−13510.
10. Weidlich, O., Schalt, B., Friedman, N., Sheves, M., Lanyi, J. K., Brown, L. S., and Siebert, F. (1996) *Biochemistry 35*, 10807−10814.
11. Yamazaki, Y., Sasaki, J., Hatanaka, M., Kandori, H., Maeda, A., Needleman, R., Shindara, T., Yoshihara, K., Brown, L. S., and Lanyi, J. K. (1995) *Biochemistry 34*, 577−582.
12. Grigorieff, N., Ceska, T. A., Downing, K. H., Baldwin, J. M., and Henderson, R. (1996) *J. Mol. Biol. 259*, 393−421.
13. Hashimoto, S., Obata, K., Takeuchi, H., Needleman, R., and Lanyi, J. K. (1997) *Biochemistry 36*, 11583−11590.
14. Dencher, N. A., Dresselhaus, D., Zaccaï, G., and Büldt, G. (1989) *Proc. Natl. Acad. Sci. U.S.A. 86*, 7876−7879.
15. Koch, M. H. J., Dencher, N. A., Oesterhelt, D., Ploehn, H.-J., Rapp, G., and Büldt, G. (1991) *EMBO J. 10*, 521−526.
16. Subramaniam, S., Gerstein, M., Oesterhelt, D., and Henderson, R. (1993) *EMBO J. 12*, 1−8.
17. Ulrich, A. S., Watts, A., Wallat, I., and Heyn, M. P. (1994) *Biochemistry 33*, 5370−5375.
18. Moltke, S., Nevzorov, A. A., Sakai, N., Wallat, I., Job, C., Nakanishi, K., Heyn, M. P., and Brown, M. F. (1998) *Biochemistry 37*, 11821−11835.
19. Earnest, T. N., Roepe, P., Braiman, M. S., Gillespie, J., and Rothschild, K. J. (1986) *Biochemistry 25*, 7793−7798.
20. Fahmy, K., Siebert, F., Grossjean, M. F., and Tavan, P. (1989) *J. Mol. Struct. 214*, 257−288.
21. Fahmy, K., Siebert, F., and Tavan, P. (1991) *Biophys. J. 60*, 989−1001.
22. Hauss, T., Büldt, G., Heyn, M. P., and Dencher, N. A. (1994) *Proc. Natl. Acad. Sci. U.S.A. 91*, 11854−11858.
23. Otto, H., and Heyn, M. P. (1991) *FEBS Lett. 293*, 111−114.
24. Schertler, G. F. X., Lozier, R., Michel, H., and Oesterhelt, D. (1991) *EMBO J. 10*, 2353−2361.
25. Ulrich, A. S., Wallat, I., Heyn, M. P., and Watts, A. (1995) *Nature Struct. Biol. 2*, 190−192.
26. Yoshida, M., Ohno, K., Takeuchi, Y., and Kagawa, Y. (1977) *Biochem. Biophys. Res. Commun. 75*, 1111−1116.
27. Otto, H., Marti, T., Holz, M., Mogi, T., Lindau, M., Khorana, H. G., and Heyn, M. P. (1989) *Proc. Natl. Acad. Sci. U.S.A. 86*, 9228−9232.
28. Sass, H. J., Schachowa, I. W., Rapp, G., Koch, M. H. J., Oesterhelt, D., Dencher, N. A., and Büldt, G. (1997) *EMBO J. 16*, 1484−1491.
29. Hu, J. G., Sun, B. Q., Bizounok, M., Hatcher, M. E., Lansing, J. C., Raap, J., Verdegem, P. J. E., Lugtenburg, J., Griffin, R. G., and Herzfeld, J. (1998) *Biochemistry 37*, 8088−8096.
30. Ohno, K., Takeuchi, Y., and Yoshida, M. (1977) *Biochim. Biophys. Acta 462*, 575−582.
31. Heyn, M. P., Westerhausen, J., Wallat, I., and Seiff, F. (1988) *Proc. Natl. Acad. Sci. U.S.A. 85*, 2146−2150.
32. Groesbeek, M. (1993) Bacteriorhodopsins and bovine rhodopsins with a modified chromophore, Ph.D. Thesis, Leiden University, Leiden, The Netherlands.
33. Oesterhelt, D., and Stoeckenius, W. (1974) *Methods Enzymol. 31*, 667−678.
34. Krebs, M. P., Mollaaghababa, R., and Khorana, H. G. (1993) *Proc. Natl. Acad. Sci. U.S.A. 90*, 1987−1991.
35. Dickopf, S., and Heyn, M. P. (1997) *Biophys. J. 73*, 3171−3181.
36. Brown, M. F. (1996) in *Biological Membranes* (Merz, K. M., Jr., and Roux, B., Eds.) pp 175−252, Birkhäuser, Basel.
37. Copié, V., McDermott, A. E., Beshah, K., Williams, J. C., Spijker-Assink, M., Gebhard, R., Lugtenburg, J., Herzfeld, J., and Griffin, R. G. (1994) *Biochemistry 33*, 3280−3286.
38. Ulrich, A. S., and Watts, A. (1993) *Solid State NMR 2*, 21−36.
39. Nevzorov, A. A., Moltke, S., and Brown, M. F. (1998) *J. Am. Chem. Soc. 120*, 4798−4805.
40. Oesterhelt, D., Tittor, J., and Bamberg, E. (1992) *J. Bioenerg. Biomembr. 24*, 181−191.
41. Urabe, H., Otomo, J., and Ikegami, A. (1989) *Biophys. J. 56*, 1225−1228.
42. Heyn, M. P., and Otto, H. (1992) *Photochem. Photobiol. 56*, 1105−1112.
43. Esquerra, R. M., Che, D., Shapiro, D. B., Lewis, J. W., Bogomolni, R. A., Fukushima, J., and Kliger, D. S. (1996) *Biophys. J. 70*, 962−970.
44. Drikos, G., and Rüppel, H. (1984) *Photochem. Photobiol. 40*, 93−104.
45. Borucki, B., Otto, H., and Heyn, M. P. (1998) *J. Phys. Chem. B 102*, 3821−3829.
46. Luecke, H., Richter, H.-T., and Lanyi, J. K. (1998) *Science 280*, 1934−1937.
47. Han, M., Groesbeek, M., Smith, S. O., and Sakmar, T. P. (1998) *Biochemistry 37*, 538−545.
48. Han, M., Groesbeek, M., Sakmar, T. P., and Smith, S. O. (1997) *Proc. Natl. Acad. Sci. U.S.A. 94*, 13442−13447.
49. Ganter, U. M., Schmidt, E. D., Perez-Sala, D., Rando, R. R., and Siebert, F. (1989) *Biochemistry 28*, 5954−5962.
50. Bloom, M., Davis, J. H., and Valic, M. I. (1980) *Can. J. Phys. 58*, 1510−1517.

BI990593U